Consecutive Rotation of Crystallographic Orientation in Lateral Growth

Mu Wang,[1,2,*] Da-Wei Li,[1] Da-Jun Shu,[1,2] Piet Bennema,[3] Yan-Wei Mao,[1] Wei Pan,[1] and Nai-Ben Ming[1]

[1]*National Laboratory of Solid State Microstructures, Nanjing University, Nanjing 210093, China*
[2]*International Center for Quantum Structures, Chinese Academy of Sciences, Beijing 100080, China*
[3]*Department of Solid State Chemistry, University of Nijmegen, 6525 ED Nijmegen, The Netherlands*

(Received 29 June 2004; published 1 April 2005)

A consecutive rotation of crystallographic orientation has been observed in lateral crystallization of NH_4Cl on a glass substrate, which induces a periodic distribution of faceted and roughened regions on the surface of a crystallite aggregate. Experimental observation indicates that this phenomenon derives from the asymmetric surface energies at the growth front, which deform the nascent nucleus and tilt the crystallographic orientation in the nucleation-mediated layered growth. We suggest that this effect is significant for a class of lateral growth where nucleation plays a dominate role.

DOI: 10.1103/PhysRevLett.94.125505 PACS numbers: 81.10.Aj, 64.60.Qb, 68.03.Cd, 82.60.Nh

The formation of thin crystalline layers on a foreign substrate, known as heteroepitaxial growth, has wide applications in materials science, physics, chemistry, and microelectronics [1,2]. Heteroepitaxial growth can usually be categorized in three distinct modes: the Volmer-Weber type, the Frank–Van der Merwe type, and the Stranski-Krastanov type [3,4]. The basic picture of interfacial growth can be summarized as the formation of islands (nucleation) first, followed by a horizontal expansion of the islands on the substrate [5,6]. Nascent islands can be compact, yet they can also be ramified and fractal-like [5–7]. As the compact islands or ramified branches develop on the substrate, the surface coverage increases and eventually a solid film is formed. Despite advances in the understanding of thin film growth, little attention has been given to effects of interfacial tensions on the horizontal expansion of a crystalline island on a foreign substrate. Especially interesting is the scenario that the lateral expansion occurs by repeated nucleation at the concave corner of the island and the substrate. Some physical properties can be significantly affected during the horizontal expansion of the islands. For example, tilting of crystallographic orientation has frequently been observed in epitaxial layers [8–10], and it was speculated that this tilting resulted from the effects of interfacial tensions. In this Letter we report on an unusual crystallization behavior of NH_4Cl on a glass substrate. We explain why the crystallographic orientation consecutively rotates in crystallization, resulting in a periodic distribution of faceted and roughened regions on the crystallite aggregate.

The crystallization was carried out in a thin layer of agarose gel containing NH_4Cl, sandwiched by two glass plates 100 μm apart. The concentrations of NH_4Cl and agarose (Merck) were 7.0 and 0.25 wt %, respectively. The supersaturation for crystallization was established by evaporating water through the edges of the glass plates [11–13]. The crystallite aggregate was observed *in situ* with a differential interference contrast (DIC) microscope (Orthoplan-pol, Leitz), and further examined *ex situ* with an atomic force microscope (AFM) (Nanoscope IIIa, Digital Instruments) in tapping mode. The orientation of crystallites in the aggregate was analyzed by micro-x-ray diffraction of synchrotron radiation (BSRF, Beijing). The point group of NH_4Cl crystal is $Pm\bar{3}m$, and NH_4^+ and Cl^- are located at $(0, 0, 0)$ and $(1/2, 1/2, 1/2)$ in the unit cell, respectively.

Instead of the zigzag branches formed at low NH_4Cl concentration [11–13], the aggregate generated at a higher initial concentration (>5.0 wt % NH_4Cl) appears random, as shown in Fig. 1. Yet striking regularity can be identified in the alternating appearance of terraces (faceted surface) and rough surface on the branch of the crystallite aggregate (Fig. 1). Suppose we establish a moving frame of coordinates on the growing front. In this moving coordinate system the crystallite surface on the very front tip of the growing aggregate changes periodically with time between faceted and roughened ones. Both micro-x-ray diffraction and micro-Raman spectroscopy confirm that the faceted surfaces are (100).

AFM reveals how the crystallographic orientation evolves in the crystallite aggregate. In Fig. 2(a) the facets

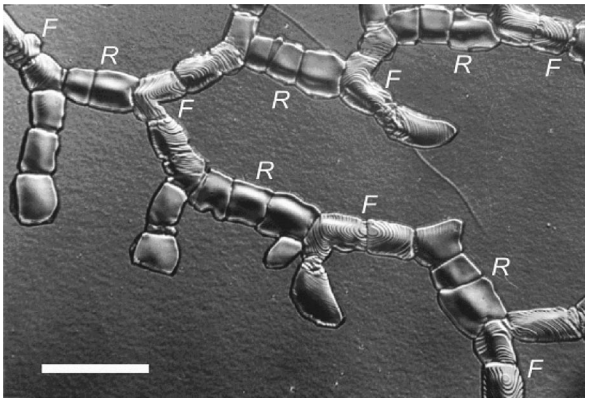

FIG. 1. The DIC micrograph of an aggregate branch of NH_4Cl crystallites, which develops from the upper-left corner towards the lower-right corner. The periodic faceted and roughened regions are marked as *F* and *R*, respectively. The bar represents 50 μm.

of crystallite A [(001) face] are in parallel with the substrate, whereas (001) on the neighboring crystallite, B, is inclined with respect to that of A. The facets on the next adjacent crystallite, C, are further tilted, as shown in Fig. 2(b). It can easily be seen that the gradual inclining of the (001) facet increases the step density on the top surface of the crystallite. When the step density becomes sufficiently high, the top surface is virtually rough, as shown in Fig. 2(c). This roughening process is different from the known thermal roughening transition and the traditional kinetic roughening transition [3,4]. The thermal roughening transition takes place when the temperature becomes higher than a critical value, and line tension of the steps vanishes. The kinetic roughening transition occurs at a sufficiently high driving force. Meanwhile the density of the nucleus becomes so high that the mean distance between the edges of the nuclei approaches the interatomic distance in scale. The roughening transition shown in Figs. 1 and 2, unlike the two aforementioned scenarios, takes place by a gradual increase of the step density on the top surface due to the continuous rotation of crystallographic orientations.

Figure 2(d) illustrates the micro-x-ray-diffraction pattern of a crystallite of type B. The elongated diffraction spots [details shown in the inset of Fig. 2(d)] indicate that, indeed, the crystallographic orientation of crystallite B changes continuously [12]. By shifting the sample with an on-site optical microscope and directing the x-ray beam onto the adjacent crystallites, respectively, along the aggregate branch, a series of Laue diffraction patterns were obtained. Analysis of the diffraction data reveals that the crystallites in Fig. 1 rotate their (001) with axis ⟨110⟩ in crystallization [14]. We can learn from Figs. 1 and 2 that not only is each piece of crystallite in the aggregate rotated a few degrees with respect to its neighbors, but the crystallographic orientation within each single-crystal-like block varies continuously as well.

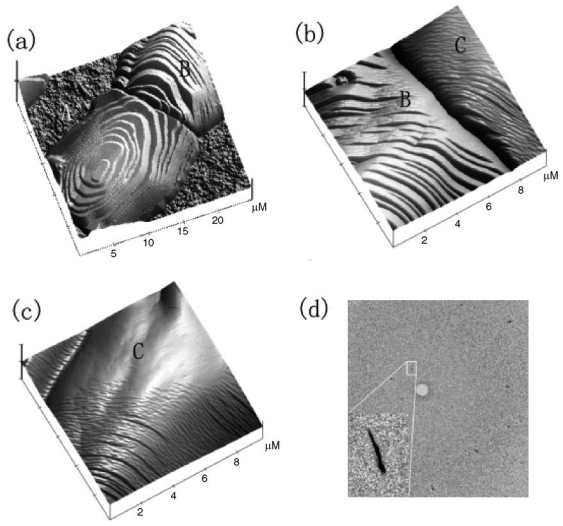

FIG. 2. (a) AFM micrograph showing that the terraces on crystallite A are nearly parallel to the substrate, and the neighboring crystallite B is oriented quite differently. (b) The next adjacent crystallite, C, is further tilted with respect to B. Hence the step density on the top surface of C becomes higher than that on B. (c) AFM micrographs of the surface of the crystallite C. At the end adjacent to crystallite B, steps can still be identified. As the crystallite develops further, the top surface transforms gradually from a stepped one to a rough one. The scale in the vertical direction (z) was 3.0 μm/div in (a)–(c). (d) The micro-x-ray-diffraction pattern of a B-type crystallite. The inset shows an enlarged elongated diffraction spot. The area of the sample illuminated by the x ray is 20 μm × 20 μm in size.

Detailed morphology of the frontmost tip of an aggregate branch is shown in Fig. 3(a), which can be regarded as a snapshot of the growing front. As indicated by the arrows, nucleation initiates from the concave corner where the crystal facet meets the substrate. During the succeeding growth, steps are continuously generated from the concave corners, propagate on the terrace, and eventually bunch to macrosteps [Fig. 3(a)]. In this way, the crystallite develops layer by layer. Actually, a bunched step with a height of about 100 nm can be identified near the site indicated by the arrow on the right side of Fig. 3(a).

Based on the facts that the Laue diffraction spots are elongated [Fig. 2(d)] and the crystallite grows layer by layer [Fig. 3(a)], we propose a mechanism for the observed phenomena as follows. The two-dimensional (2D) nucleation rate can be expressed as $J_0 = \omega^* \Gamma C \times \exp(-\Delta G^*/k_B T)$, where Γ is known as the Zeldovich factor, ω^* is the attaching frequency of molecules to the nucleus, C is the local concentration, and ΔG^* is the energy barrier for nucleation [4]. It follows that the 2D-nucleation rate can be written as

$$\ln J_0 = a - b\left(\frac{\Delta\mu}{k_B T}\right)^{-1}, \tag{1}$$

where $\Delta\mu$ is the difference of the chemical potential between a molecule in crystalline phase and the same molecule in aqueous solution; parameters a and b, which are related to the kinetic process and the thermodynamic barrier, are determined by surface or interface tensions, flux of molecules towards the growing front and temperature [14]. Now we consider, respectively, the nucleation rate on the crystal facet away from the edges [scenario 1 in Fig. 3(b)] and the nucleation rate at the concave corner, where the nucleus contacts both the crystal facet and the glass substrate [scenario 2 in Fig. 3(b)]. In scenario 2, strain is involved in nucleation because the underlying substrate is inhomogeneous in surface energy: in effect, one part of the substrate is the crystal facet, whereas the other part is the glass substrate. The inhomogeneous surface energies may generate a torque to deform the embryonic nucleus. It has been well established that in a metallic thin film the nanocrystallites may have rotated crystallographic orientations, leading to the coalescence of neighboring grains [15]. In that case the driving force for grain rotation is the cumulative torque related to the length of the individual grain boundary. In our case, a similar situation

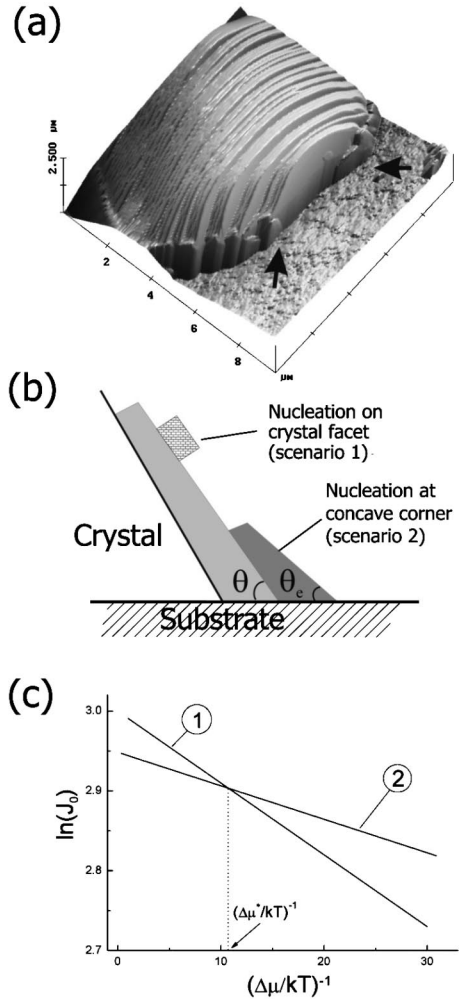

FIG. 3. (a) AFM view of the very front tip of an aggregate branch. Nucleation appears at the concave corner of the crystal facet and the glass substrate, which acts as the step source, as indicated by the arrows. The crystal develops forward layer by layer. (b) A schematic illustration of two possible nucleation sites on the growth front. For scenario 1, a new nucleus appears on the crystal facet. For scenario 2, nucleation takes place at the concave corner. The asymmetric interfacial tensions at the corner deform (rotate) the nucleus. Hence a strained crystalline layer is formed. Thereafter, a new nucleus appears at the concave corner and the previous process repeats. (c) A graph to illustrate the relation of the nucleation rate and $(\Delta\mu/k_{\max}T)^{-1}$. Line 1 corresponds to scenario 1, and line 2 corresponds to scenario 2 (the strained case). It can be seen that there exists a critical value $\Delta\mu^*$, below which the cycle of strained nucleation at the reentrant corners is favored.

occurs to the nascent nucleus at the concave corner: the unbalanced interfacial tensions either rotate or deform the embryo. In this way, strain is introduced to the crystallite. From the detailed expression of b, we expect that b in scenario 2 is smaller compared with that in scenario 1 [14]. The nucleation rates are schematically plotted as a function of $(\Delta\mu/k_{\mathrm{B}}T)^{-1}$ in Fig. 3(c). There exists a critical driving force $\Delta\mu^*$, below which the nucleation rate for scenario 2 becomes always higher than that for scenario 1. This means that nucleation at the concave corner, although strained, remains thermodynamically favorable since the contribution of the surface or interface tensions may overwhelm the effect of strain at the concave corner in nucleation. Further, our calculation indicates that the tilting of (001) of the nucleus with respect to the adjacent (001) crystalline facet [i.e., $(\theta_e - \theta)$ in Fig. 3(b)] does not change sign in the crystallization process and is proportional to $\Delta\mu$ [14]. This is consistent with our experimental observations, where the rotation of the crystallographic orientation always follows a certain direction.

The above interpretation is supported by an *in situ* optical observation. It is known that if strain (stress) is involved in crystallization, the crystallite surface will be destabilized when a certain size is reached. It is known that a nominally flat surface profile of an elastically stressed solid can rapidly evolve into a cusped surface, with smooth tops and deep cracklike grooves by surface diffusion [16,17]. Comparing with conventional Mullins-Sekerka instability [3,4], which is driven by diffusion and takes place at a long wavelength, the instability presented here is also a long-wavelength instability, but it is driven by stress [16–19]. The characteristic length of the surface pattern can be estimated by $k_{\max}$, the upper limit of the linearly unstable wave vector. Suppose the crystal is subjected to a uniaxial stress, and the strain is ϵ_{xx}, it follows that the critical unstable wavelength is

$$\lambda_0 = \frac{2\pi}{k_{\max}} = \frac{\pi\gamma(1-\sigma^2)}{E\epsilon_{xx}^2}, \tag{2}$$

where E is the Young's modulus of the material, σ the Poisson coefficient, and γ the surface tension of the crystal. From the elongation of the Laue diffraction spots, we know that the crystallographic orientation of each individual crystallite has been rotated about 3°. The lateral size of the crystallite is of the order of 20 μm, and the height of the crystallite is about 2 μm. It follows that the strain inside the crystallite will be on the order of 1.8×10^{-3}. This value, together with the elastic data of the NH_4Cl crystal [20], yields $\lambda_0 \sim 36$ μm according to Eq. (2). This means that when the size of a crystallite reaches λ_0, its top surface becomes unstable. Hence wrinkles will develop on the surface of the crystallite. The evolution of the wrinkles results in a ditch and finally separates the crystallite [21]. This scenario has, indeed, been experimentally observed. As illustrated in Figs. 4(a) and 4(b), when the crystallite on the tip of the aggregate branch develops to a certain size, wrinkles emerge on the crystallite surface [marked by the dark arrow in Fig. 4(b)]. The wrinkles move in a restricted region and bunch into a long, deep ditch. Eventually the crystallite is separated [Fig. 4(c)]. Thereafter, as the separated crystallite on the branch tip grows forward, wrinkling reappears as soon as a certain length is reached, as indicated by the white arrow in Fig. 4(d). By repeating this elongation-wrinkling-separation process, an aggregate of crystallites such as that shown in Fig. 1 is formed. Our ex-

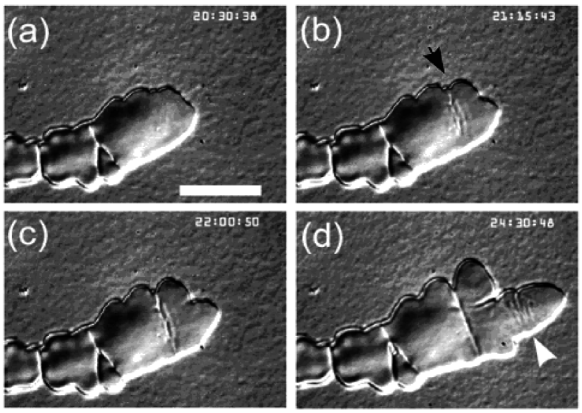

FIG. 4. *In situ* DIC micrographs showing the formation of the aggregate of NH_4Cl crystallites. At a certain size, wrinkles emerge on the surface of the frontmost crystallite [shown by the black arrow in (b)]. (b),(c) The wrinkles eventually bunch into a ditch and separate the crystallite. (d) As the new frontmost crystallite grows further, as soon as the critical length is reached, new wrinkles reappear. Repeating this process leads to the pattern shown in Fig. 1. The digits in the time scale represent minute, second, and 1/100 s, respectively. The bar represents 25 μm.

periments also show that the spatial periodicity on the aggregate branch depends on supersaturation. At higher supersaturation, the nucleation rate is higher and crystal grows faster. Consequently, the size of crystallite becomes smaller (indicating that the strain accumulation rate is faster) and the spatial periodicity on the aggregate surface is shorter. For lower supersaturation, crystallite becomes larger (strain accumulates slowly in crystallization), hence the spatial periodicity on the aggregate becomes longer. This observation further supports our understanding that the phenomena reported in this Letter are indeed strain related.

Nowadays in thin film growth people usually focus on the increase of film thickness, and little attention has been paid to the lateral extension of a crystalline island on a foreign substrate. Here we demonstrate for the first time that once a crystallite develops laterally on a foreign substrate and the crystallization is promoted by successive nucleation at the concave corner of the crystal facet and the substrate, the newborn nucleus will be strained and its crystallographic orientation will be continuously rotated. The physical reason for this effect is the asymmetry of the surface energies at the concave corner of the crystallite and the foreign substrate, which keeps deforming the nucleus embryo there. Our micro-x-ray-diffraction studies show that if crystallite initially contacts the substrate with its (111) face, and rotates with $\langle 110 \rangle$ as the axis, a regular zigzag branch develops along $\langle 1\bar{1}0 \rangle$ as that reported in Refs. [11–13]. If, however, the crystallite initially contacts the substrate with its (001) face and rotates with $\langle 110 \rangle$ as the axis, the periodic distribution of faceted regions and rough regions on the aggregate (Fig. 1) will be observed. We emphasize that, although we concentrate in this Letter on crystallization of NH_4Cl, similar growth behavior has, indeed, been observed in the crystallization of CsCl, $FeSO_4$, $Ba(NO_3)_2$ [22], and some bioagents [23]. Since the asymmetric surface tensions at the concave corner always exists in heteroepitaxial growth, and normally nucleation at the concave corner is thermodynamically favored, we expect that the phenomenon reported in this Letter may have a general importance for nucleation-mediated lateral growth and would benefit many areas of condensed matter science.

The authors acknowledge financial support from NSFC (10374043, 10021001, and 90201039) and Ministry of Science and Technology (2004CB619005). The authors thank the Station of X-Ray Topography on the beam line 4W1A of BSRF for the help with diffraction experiments, and V. Fleury, J.-F. Gouyet, M. Plapp, Z. Y. Zhang, and F. Liu for discussions.

*To whom correspondence should be addressed.
Electronic address: muwang@nju.edu.cn

[1] A. A. R. Elshabini-Riad and F. D. Barlow, *Thin Film Technology Handbook* (McGraw-Hill Professional, New York, 1997).
[2] *Thin Films: Preparation, Characterization, Applications*, edited by M. P. Soriaga (Plenum Publishing Corp., New York, 2002).
[3] A. Pimpinelli and J. Villain, *Physics of Crystal Growth* (Cambridge University Press, Cambridge, 1998).
[4] I. V. Markov, *Crystal Growth for Beginners: Fundamentals of Nucleation, Crystal Growth and Epitaxy* (World Scientific, Singapore, 1995).
[5] H. Brune, C. Romainczyk, H. Roder, and K. Kern, Nature (London) **369**, 469 (1994).
[6] F.-J. M. zu Heringdorf, M. C. Reuter, and R. M. Tromp, Nature (London) **412**, 517 (2001).
[7] Z. Zhang and M. G. Lagally, Science **276**, 377 (1997).
[8] P. Fini *et al.*, Appl. Phys. Lett. **76**, 3893 (2000).
[9] T. M. Katona *et al.*, Appl. Phys. Lett. **79**, 2907 (2001).
[10] A. J. Steinfort *et al.*, Phys. Rev. B **57**, 12 530 (1998).
[11] M. Wang *et al.*, Phys. Rev. Lett. **80**, 3089 (1998).
[12] D.-W. Li *et al.*, J. Phys. Chem. B **107**, 96 (2003).
[13] X. Y. Liu *et al.*, J. Cryst. Growth **208**, 687 (2000).
[14] D. J. Shu *et al.* (to be published); and in supplementary material.
[15] D. Moldovan, D. Wolf, and S. R. Phillpot, Acta Mater. **49**, 3521 (2001); D. Moldovan, V. Yamakov, D. Wolf, and S. R. Phillpot, Phys. Rev. Lett. **89**, 206101 (2002).
[16] J. Berrhar *et al.*, Phys. Rev. B **46**, 13 487 (1992).
[17] W. H. Yang and D. J. Srolovitz, Phys. Rev. Lett. **71**, 1593 (1993).
[18] R. J. Asaro and W. A. Tiller, Metall. Trans. **3**, 1789 (1972).
[19] M. A. Grinfeld, Sov. Phys. Dokl. **31**, 831 (1986).
[20] B. Winkler *et al.*, J. Phys. Condens. Matter **12**, 2093 (2000).
[21] J. Muller, Ph.D. thesis, McGill University, 1998.
[22] M. Wang *et al.* (to be published).
[23] See, for example, the cover picture of Laborwelt **4**, No. 5 (2003).